CONF-9610242--1

A COUPLED MONTE CARLO-FINITE ELEMENT APPROACH TO MODELING MICROSTRUCTURAL EVOLUTION DURING STATIC RECRYSTALLIZATION*

G. Sarma, B. Radhakrishnan and T. Zacharia

Oak Ridge National Laboratory, P.O. Box 2008, MS 6140, Oak Ridge, TN 37831-6140, USA

ABSTRACT

A novel methodology is presented for modeling static recrystallization in metals, by combining the finite element simulation of cold deformation with the Monte Carlo simulation of recovery and grain growth. A model based on crystal plasticity is used to simulate the deformation of an aggregate of grains, so as to capture the inhomogeneous deformation of individual grains, and the strain hardening and texture evolution in the aggregate. The non-uniform distributions of orientation and stored energy are then mapped onto a Monte Carlo grid for simulating static recrystallization. The method has been applied to compute the kinetics and microstructural evolution after different amounts of cold deformation, and leads to improved predictions due to the use of more realistic data in the Monte Carlo simulations.

INTRODUCTION

In the last decade, there has been a great deal of activity in modeling the microstructural evolution during recrystallization using the Monte Carlo (MC) technique at the mesoscopic level [1–4]. In this approach, the continuum microstructure is mapped onto a discrete MC grid. Each grain is represented by a collection of grid points with the same orientation number, with grain boundaries being assumed to exist between points with unequal numbers. In these simulations [1–3], the nucleation phenomenon is not modeled explicitly. Rather, nuclei are added arbitrarily to the microstructure either at the start of the simulation to capture site saturation effects, or continuously as a function of simulation time to model constant nucleation

rate effects. To simulate the recrystallization process, each of the MC sites is visited in a random fashion, and the change in energy for flipping a site from cold worked state to recrystallized state is computed, with the change being favored only if it leads to a reduction in the energy.

This article describes a novel technique for modeling static recrystallization by combining a finite element (FE) simulation of the cold deformation with the MC approach for treating recovery and recrystallization. By means of explicit discretization of grains at the microstructural level, the FE analysis permits modeling the inhomogeneous deformation of the grains to predict changes in the grain shape, orientation and stored energy distributions. A constitutive model based on crystal plasticity enables modeling the hardening and texture evolution under the applied deformation. The MC approach treats recrystallization in the usual manner as described above. However, an important difference is that each MC site is now assigned a unique value of crystallographic orientation and stored energy of deformation. The availability of quantitative information about the cold worked microstructure in terms of the stored energy and orientation distributions permits an explicit modeling of the nucleation step by the growth of subgrains in the presence of an orientation gradient.

COUPLED FE-MC MODEL FOR RECRYSTALLIZATION

Finite Element Model for Deformation: The details of the FE formulation are given elsewhere [5,6], and only a brief description is provided here. The approach consists of discretizing a polycrystalline aggregate with finite elements, so that each grain is made up of several hundred elements, and applying boundary conditions corresponding to a homogeneous deformation to the aggregate. Balance laws for equilibrium and conservation of mass are used to solve for the material motion at each strain increment, keeping the state and geometry fixed. Upon obtaining a converged solution for the velocity field, the material state and geometry are updated. Following the approach described in Beaudoin *et al.* [5], a hybrid finite element formulation is employed for computing the discretized velocity field, where the equilibrium statement is developed in a weighted residual sense from a balance of tractions at element interfaces. This approach is advantageous in handling the abrupt changes in element properties, especially across grain boundaries.

In each element, the material state is described by its orientation and its hardness (critical resolved shear stress on the slip systems). The anisotropic material response of the element is determined by its current state. The symmetric part of the velocity gradient (rate of deformation) is used to compute the shearing rates on the individual slip systems in an element [7]. The difference between the skew-symmetric part of the velocity gradient (spin) and the plastic spin due to shearing of slip planes drives the reorientation of the crystal. The hardness values are updated based on the sum of the slip system shearing rates using a modified Voce law [7].

Use of crystal plasticity and a hybrid finite element formulation lead to a significant increase in the computational burden associated with the material property calculations. However, a proper choice of interpolation functions enables exploitation of parallel computing technologies, which in turn permits treatment of large three-dimensional discretizations. The formulation has been implemented on the Intel PARAGON parallel computer using High Performance Fortran (HPF) [6].

Monte Carlo Model for Recrystallization: The first step in the MC simulations is the mapping of the stored energy and orientation distributions obtained from the FE deformation model onto the MC grid. An important consideration is that information must be transferred from

DISCLAIMER

a distorted FE mesh to a regular MC grid. A cubic grid is used for the MC simulations. The stored energy per unit volume H of a site is given by [8]

$$H = \frac{2\hat{\tau}^2}{\mu}, \tag{1}$$

where $\hat{\tau}$ is the slip system critical resolved shear stress for the element, and μ is the shear modulus of the material. The dislocation substructure at each MC site is assumed to be made up of a collection of subgrains. The mean subgrain size D_0 for a given deformation is obtained from the experimental data compiled by Gil Sevillano *et al.* [9]. The average misorientation θ_0 between the subgrains at each MC site is calculated using the following relation [8]:

$$H = \frac{2\gamma_m}{D_0}\frac{\theta_0}{\theta^*}\left[1 - \ln\left(\frac{\theta_0}{\theta^*}\right)\right], \tag{2}$$

where γ_m is the high angle boundary energy, and θ^* is the misorientation limit for low angle boundaries (assumed to be 15° in the simulations). The growth of the subgrains at each MC site is calculated using the equation

$$\frac{dD}{dt} = \frac{\theta}{\theta^*}\left[1 - \ln\left(\frac{\theta}{\theta^*}\right)\right]\frac{k}{D}, \tag{3}$$

where D is the subgrain size at time t, and k is the mobility of the subgrain boundaries. In the simulations k was treated as an adjustable parameter so that active nuclei could be obtained in a reasonable number of MC time steps (MCS). Furthermore, it is assumed that the cell size D depends linearly on the misorientation θ among subgrains according to

$$\frac{\theta - \theta_0}{D - D_0} = \frac{\theta_{av} - \theta_0}{L - D_0}, \tag{4}$$

where θ_{av} is the average misorientation between each MC site and its neighboring sites. Equation (4) implies that the misorientation between the subgrains becomes equal to the average misorientation between the site and its neighbors when the subgrain size becomes equal to the size of the lattice site L. The subgrain misorientation is calculated at each time step by simultaneously solving equations (3) and (4), and the MC site is declared as a nucleus when the average misorientation between the subgrains exceeds θ^*.

The average energy of a MC site decreases as a result of subgrain growth because of the reduction in the total surface area of the subgrain boundaries per unit volume. The energy per unit volume as a function of subgrain size is obtained using equation (2), after replacing θ_0 with θ and D_0 with D. When the misorientation θ exceeds θ^*, the energy per unit volume of the sites is calculated as

$$H = \frac{2\gamma_m}{D}. \tag{5}$$

The reduction of the site energy as a function of the simulation time accounts for the recovery process which occurs during recrystallization. In the simulations, each MC site is visited in a random fashion. If the visited site is unrecrystallized, then one if its six nearest neighbors is picked at random as the flip-site. If the flip-site is also unrecrystallized, then the nucleation model described previously is applied to the visited site. If the flip-site is recrystallized, then the possibility of flipping the visited unrecrystallized site to the recrystallized flip-site is considered

by estimating the local energy change as a result of flipping the site, with the flip being allowed only when the local energy change is less than or equal to zero. When the visited site is a recrystallized site, there are two possibilities. The flip-site can be either recrystallized or unrecrystallized. The latter case is not applicable, since it would lead to an increase in the local energy. The former case corresponds to the curvature driven migration of high angle boundaries. However, grain growth is not considered in the present simulation.

APPLICATION TO SIMULATION OF STATIC RECRYSTALLIZATION

The methodology discussed in the previous section has been used to simulate the cold deformation and subsequent recrystallization stages. Two different cold reductions corresponding to plastic strains of $e = 0.7$ and $e = 1.1$ were simulated using appropriate discretizations and material parameters for 1100 aluminum [7]. A 3-D MC grain growth simulation [10] was used to obtain the initial microstructure for the FE calculations. For $e = 0.7$ a mesh of $15\times30\times60$ elements was initialized with random orientations using a one-to-one correspondence between the elements and the grid points after grain growth. In a similar fashion, the $e = 1.1$ case was simulated using a mesh of size $10\times30\times90$. The initial mesh in each case was made up of elements which were cubes, so that the overall domain was a parallelepiped with sides in the same proportion as number of elements in each direction.

Boundary conditions were applied to the mesh such that the material deformed in plane strain compression at constant unit deformation rate. After deformation, the aspect ratio of the overall mesh became 1:1:1. The individual elements, which started as cubes, elongated in the x-direction and reduced in length along the z-direction in the ratio of the number of elements along each direction. Since the MC grid points required uniform spacing in the three directions to avoid any bias in the mobility of grain boundaries, the following scheme was utilized in mapping information from the finite elements. Since there were greater numbers of elements along z than along x, for $e = 0.7$, two points were placed in an element along the x-direction for every point along y and z, while only one in two elements was used along the z-direction. In similar fashion, points were repeated three times along x, and one in three elements was used along z for $e = 1.1$. The values at the element centroid were used in the MC simulations for initializing the stored energy and orientation at grid points from the chosen elements.

RESULTS AND DISCUSSION

Figure 1 shows the recrystallization kinetics after plastic strains of 0.7 and 1.1, with larger strain leading to faster kinetics. While the recrystallization is essentially complete for $e = 1.1$, the recrystallized fraction (f_{rex}) is only 0.9 for $e = 0.7$. Figure 2 shows a plot of $\ln[\ln\{1/(1-f_{rex})\}]$ as a function of ln(MCS) for the data shown in Figure 1. For ideal Johnson-Mehl-Avrami-Kolmogorov (JMAK) behavior [8], this plot results in a straight line. However, in this case there are significant deviations form ideal JMAK behavior for both strain levels.

Figure 3 shows the evolution of the surface area per unit volume (S_v) of the boundaries between the recrystallized and un-recrystallized portions of the microstructure. S_v initially increases with f_{rex}, before reaching a maximum and then decreasing to zero when the recrystallization nears completion. There are significant differences in the variation of the S_v with f_{rex} for $e = 0.7$ and $e = 1.1$. At lower plastic strain, S_v attains a maximum value of 0.2 μm^{-1} at a volume fraction of 0.3, while for $e = 1.1$, the maximum S_v is 0.36 μm^{-1} when f_{rex} is 0.45. Also, the S_v curve for the lower strain is less symmetric, with a sharp ascent followed by a more gradual decline.

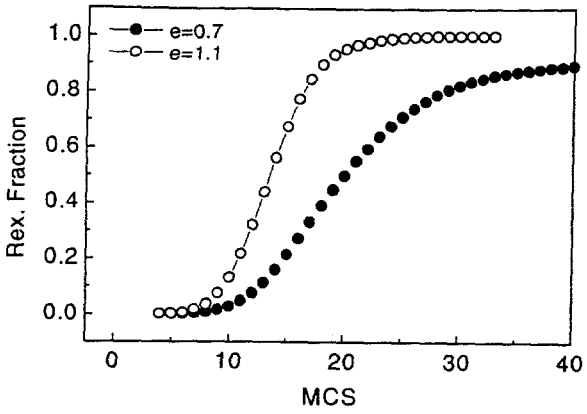

Figure 1. Variation of recrystallized volume fraction with MCS.

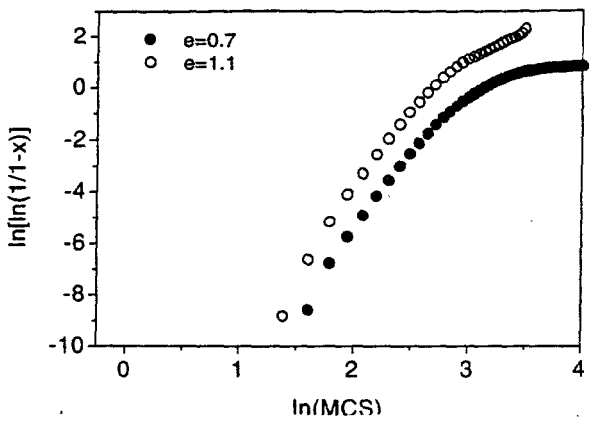

Figure 2. Variation of $\ln[\ln\{1/(1-f_{rex})\}]$ with ln(MCS).

Figure 4 shows the total number of nuclei as a function MCS for the two strains, with $e = 1.1$ leading to more than twice as many nuclei as $e = 0.7$. The nucleation rate drops to zero at MCS of 18 for $e = 0.7$ and MCS of 13 for $e = 1.1$. From Figure 1, it is observed that at these values of MCS the curve for f_{rex} shows an inflexion, and the values of f_{rex} (0.3 for $e = 0.7$ and 0.45 for $e = 1.1$) correlate with those at which S_v reaches a maximum in Figure 3.

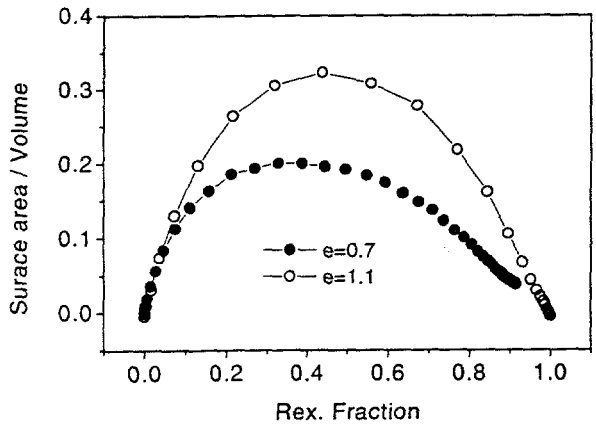

Figure 3. Evolution of S_v (see text) with recrystallized volume fraction.

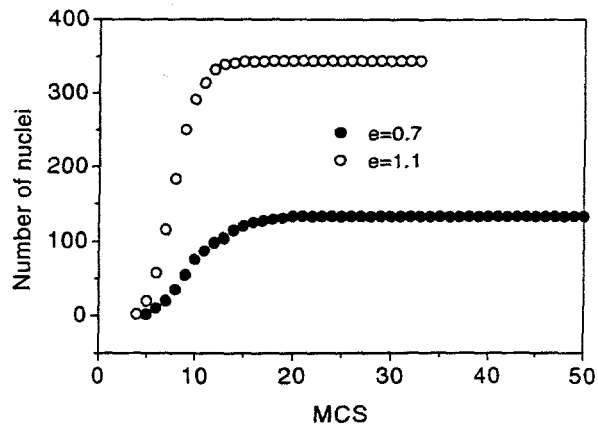

Figure 4. Variation of total number of nuclei with MCS.

Figure 5(a) shows a section normal to the y-direction of the initial microstructure prior to cold deformation from the 15×30×60 grid. Figure 5(b) shows the strain energy distribution in the microstructure after deformation, mapped to the original grid. Note that the stored energy in regions close to prior grain boundaries is higher than in the grain interior. Figure 5(c) shows the distribution of the nucleation parameter ν, defined as the product of the stored energy and average misorientation of a MC site with its nearest neighbors after deformation, mapped to the original grain structure. Comparing Figures 5(a) and 5(c), it is clear that ν is maximized in the vicinity of prior grain boundaries and triple junctions. A systematic examination of the entire simulation volume by serial sectioning showed that ν was also high at certain interior locations of coarse grains, indicating the formation of deformation bands in the microstructure.

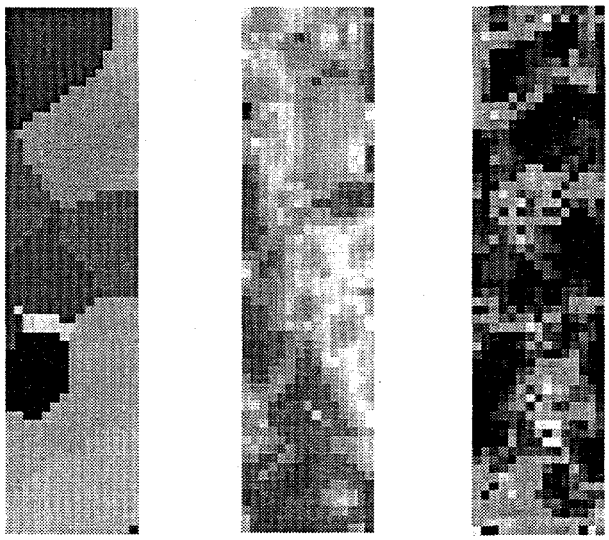

Figure 5. Stored energy and nucleation parameter mapped to the original microstructure.

Figure 6 shows the temporal evolution of the microstructure for $e = 0.7$ for one of the sections. Also shown in Figure 6 are the deformed grain structure and the distribution of the nucleation parameter. There is clearly a one-to-one correlation between the nucleation sites and the sites for which ν has a high value. Figure 6 also shows that for $e = 0.7$, the nucleation occurs in a non-random fashion. This is due to the fact that the nucleation parameter is maximized at specific locations such as prior grain boundaries and triple points. Intragrain nucleation also occurs in a non-random fashion at the deformation bands. Non-random nucleation leads to early impingement of the recrystallization fronts originating from these nuclei. From Figure 6, it is clear that the impingement is quite significant at MCS of 17. Beyond this stage the nucleation rate is almost zero, causing S_v to decrease since the loss of surface area due to impingement is greater than the surface area created by nucleation. Non-random nucleation also causes impingement to occur preferentially in certain directions, and hence the rate of decrease of S_v is lower than for uniform impingement.

Figure 7 shows the microstructural evolution for $e = 1.1$, along with the deformed grain structure and the distribution of the nucleation parameter. Once again, there is a one-to-one correlation between the nucleation sites and the sites with high values of ν. Figure 7 shows that the nucleation is more random than at the lower strain, resulting in delayed impingement of the recrystallization fronts. The increased nucleation rate at $e = 1.1$ compared to $e = 0.7$ results in a finer recrystallized grain size, as seen from Figures 6 and 7. The increased nucleation rate at the larger strain is essentially due to two factors. The initial average subgrain size D_0 at the MC sites decreases with increasing deformation. From equation (2), this results in a greater initial misorientation between the subgrains. Equation (2) also shows that the initial misorientation between subgrains increases with larger stored energy of deformation. Since the total time for recrystallization is reduced compared to $e = 0.7$, the time available for recovery is also reduced. Hence, the recrystallization goes to 100% completion. However, the latter stages of recrystallization do occur at a reduced rate, as indicated by the change of JMAK slope in Figure 2.

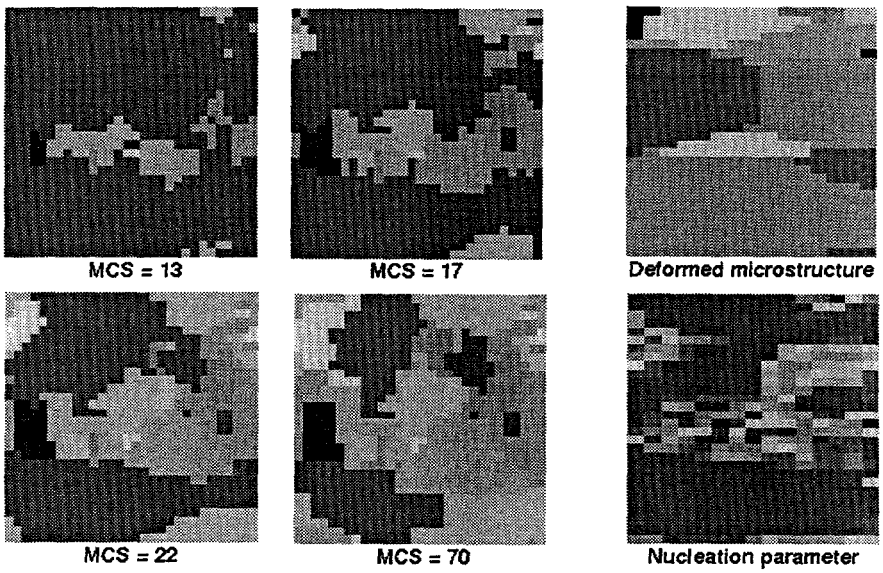

Figure 6. Temporal evolution of recrystallized microstructures for $e = 0.7$ (left) and correlation with nucleation parameter (right).

An important contribution of the present research is the development of a nucleation model for recrystallization from first principles, based on the quantitative description of stored energy and orientation distributions in the cold worked microstructure obtained from the finite element model. The total number of active nuclei during recrystallization for $e = 0.7$ and $e = 1.1$ are 133 and 344, respectively. Hence, it is clear that only a small fraction of the sites in the cold worked microstructure has managed to become nuclei in both cases. This is because the potential for nucleation at a given site depends not only on the stored energy at the site but also on the presence of a local orientation gradient in the vicinity of the site [11]. Hence, although the grain boundary and triple point sites as well as sites in a shear band within a grain can potentially become nuclei, the sites that eventually become active nuclei are only those around which significant local orientation gradients also exist.

CONCLUSIONS

A novel technique has been developed for modeling static recrystallization in metals by coupling a Monte Carlo simulation with a finite element deformation model based on crystal plasticity. A model based on subgrain growth in the presence of local orientation gradients has been developed for treating the nucleation step and has been successfully integrated with the MC recrystallization model. The coupled FE-MC model has been used to predict the effect of prior deformation on the recrystallization kinetics and the microstructural evolution. Due to the non-uniform distribution of stored energy among the MC sites, significant deviations from ideal JMAK behavior were observed for the different strain levels. Larger deformation lead to faster kinetics and a greater number of total nuclei. A nucleation parameter defined as the product of the stored energy with the average misorientation of a site with its nearest neighbors was used to correlate the sites where nucleation occured with high values of ν. Due to greater heterogeneity in the distribution of ν, nucleation occured in a less random manner for $e = 0.7$ compared to $e = 1.1$. The preferential nucleation lead to early impingement of the recrystallization fronts, and a lower rate of decrease of S_v compared to the more uniform impingement at $e = 1.1$. It was observed that the recrystallized volume fraction at which S_v

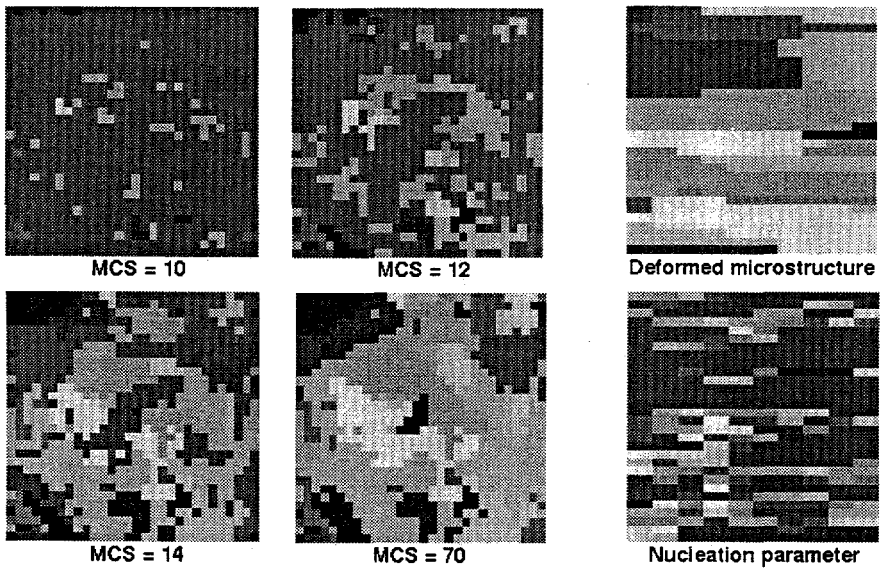

Figure 7. Temporal evolution of recrystallized microstructures for $e = 1.1$ (left) and correlation with nucleation parameter (right).

reaches a maximum is obtained when the rate of nucleation drops to zero.

ACKNOWLEDGMENTS

This research was sponsored by the Division of Materials Science, U.S. Department of Energy, under contract DE-AC05-96OR22464 with Lockheed Martin Energy Research Corporation. The research was supported in part by an appointment to the Oak Ridge National Laboratory Postdoctoral Research Associates Program administered jointly by the Oak Ridge National Laboratory and the Oak Ridge Institute for Science and Education. The authors acknowledge the use of the Intel PARAGON XP/S 35 located in the Oak Ridge National Laboratory Center for Computational Sciences (CCS), funded by the Department of Energy's Office of Scientific Computing. The authors thank Drs. S.S. Babu and J.H. Schneibel for reviewing the article.

REFERENCES

1. D.J. Srolovitz, G.S. Grest and M.P. Anderson, Acta Metall., 34, 1986, p. 1833.
2. D.J. Srolovitz, G.S. Grest, M.P. Anderson and A.D. Rollett, Acta Metall., 36, 1988, p. 2115.
3. A.D. Rollett, D.J. Srolovitz, M.P. Anderson and R.D. Doherty, Acta Metall. Mater., 40, 1992, p. 3475.
4. B. Radhakrishnan, Oak Ridge National Laboratory, 1996, unpublished research.
5. A.J. Beaudoin, P.R. Dawson, K.K. Mathur and U.F. Kocks, Int. J. Plast., 11, 1995, p. 501.
6. G. Sarma, T. Zacharia and D. Miles, Comp. and Math. with Applic., 1996, submitted.
7. K.K. Mathur and P.R. Dawson, Int. J. Plast, 5, 1989, p. 67.
8. F.J. Humphreys and M. Hatherly, Recrystallization and Related Annealing Phenomena, Elsevier, Oxford, U.K., 1995.
9. J. Gil Sevillano, P. van Houtte and E. Aernoudt, Prog. Mater. Sci., 25, 1980, p. 69.
10. B. Radhakrishnan and T. Zacharia, Metall. Mater. Trans. A, 26, 1995, p. 167.
11. I.L. Dillamore, P.L. Morris, C.J.E. Smith and W.B. Hutchinson, Proc. Roy. Soc. Lond. A, 329, 1972, p. 405.